THE ASTROPHYSICAL JOURNAL, 534:258–264, 2000 May 1

INTEGRATING THE *BeppoSAX* GAMMA-RAY BURST MONITOR INTO THE THIRD INTERPLANETARY NETWORK

K. HURLEY
University of California, Berkeley, Space Sciences Laboratory, Berkeley, CA 94720-7450; khurley@sunspot.ssl.berkeley.edu

M. FEROCI, M.-N. CINTI, E. COSTA, AND B. PREGER
Istituto di Astrofisica Spaziale/Consiglio Nazionale delle Ricerche, Rome, I-00133 Italy

F. FRONTERA, D. DAL FIUME, M. ORLANDINI, AND L. AMATI
Istituto di Tecnologie e Studio delle Radiazioni Extraterrestri, Bologna, Italy

L. NICASTRO
Istituto di Fisica Cosmica e Applicazioni dell'Informatica, Palermo, Italy

J. HEISE AND J. J. M. IN 'T ZAND
Space Research Organization Netherlands, Utrecht, Netherlands

AND

T. CLINE
Goddard Space Flight Center, Code 661, Greenbelt, MD, 20771
Received 1999 July 14; accepted 1999 December 17

ABSTRACT

We have added the *BeppoSAX* Gamma-Ray Burst Monitor to the third Interplanetary Network (IPN3) of burst detectors. We analyze 16 bursts whose positions are known to good accuracy from measurements at other wavelengths. We show that there is excellent agreement between the *Ulysses*/*BeppoSAX* triangulation annuli and the known positions of these events and that these annuli can in many cases provide useful constraints on the positions of bursts detected by the *BeppoSAX* Wide-Field Camera and Narrow-Field Instruments.

Subject heading: gamma rays: bursts

1. INTRODUCTION

It is now well known that the breakthrough in our understanding of cosmic gamma-ray bursts (GRBs) has come about through the multiwavelength identification of fading counterparts and that this revolution was initiated by *BeppoSAX* observations and precise localizations of X-ray counterparts (e.g., Costa et al. 1997) with the Wide-Field Camera (WFC). Less well known, however, is the fact that *BeppoSAX* has other ways of localizing bursts, in particular with the Gamma-Ray Burst Monitor (GRBM). Here we describe the results of integrating *BeppoSAX* into the third Interplanetary Network of GRB instruments and demonstrate that triangulation using the GRBM and *Ulysses* is capable of producing precise localization annuli whose accuracy can be verified using the locations of GRB counterparts determined from observations at other wavelengths.

2. INSTRUMENTATION

The *BeppoSAX* GRBM (Feroci et al. 1997; Amati et al. 1997; Frontera et al. 1997) is the anticoincidence shield for the Phoswich Detection System. Briefly, this shield consists of four optically independent CsI(Na) scintillators, each 1 cm thick, 27.5 cm high, and 41.3 cm wide. Although the geometric area of a shield element is 1136 cm^2, the maximum effective area for a burst with a typical power-law spectrum, arriving at normal incidence, is about 420 cm^2 for units 1 or 3 (the optimum units) when shadowing by spacecraft structures and the detector housing are taken into account. The GRBM records data in either a triggered or a real-time mode, in the energy range $\sim$40–700 keV. In the triggered mode, time resolutions up to 0.48 ms are available; in the real-time mode, the resolution is 1 s. For a triggered event, real-time data are also transmitted. As the spacecraft is in a near-equatorial orbit, it benefits from a very stable background.

The *Ulysses* GRB detector (Hurley et al. 1992) consists of two 3 mm thick hemispherical CsI(Na) scintillators with a projected area of about 20 cm^2 in any direction. The detector is mounted on a magnetometer boom far from the body of the spacecraft and therefore has a practically unobstructed view of the full sky. Because the *Ulysses* mission is in interplanetary space, the instrument also benefits from an exceptionally stable background. The GRB detector operates continuously, and over 97% of the data are recovered. The energy range is $\sim$25–150 keV, and like the GRBM, it takes data in both triggered and real-time modes, with time resolutions as fine as 8/1024 ms and as coarse as 2 s. Also, like the GRBM, real-time data are transmitted for triggered events.

3. SCOPE OF THIS WORK

Because of the very different sensor areas, thicknesses, and energy ranges, it is not immediately obvious that burst time histories from these two instruments can be cross-correlated accurately, a prerequisite for precise triangulation. (The triangulation technique is described in detail in Hurley et al. 1999a.) Our goal in this paper is to demonstrate that this is indeed the case. To accomplish this, we have selected bursts according to the following criteria:

1. The burst must have been observed by both *Ulysses* and the *BeppoSAX* GRBM, in either triggered or real-time data modes;
2. The burst must have been independently localized to an accuracy equal to or better than that achieved by tri-

TABLE 1

BeppoSAX Gamma-Ray Burst Monitor/*Ulysses* Gamma-Ray Bursts

Date	UT (s)[a]	*Ulysses* Data	GRBM Data	Other Observations[b]
1997 Jan 11	35040	T[c]	T	BATSE #5773, Konus, *DMSP*, WFC
1997 Feb 28	10681	T	T	Konus, WFC
1997 Apr 2	80379	R[d]	R	Konus, WFC
1997 May 8	78050	R	T	BATSE #6225, Konus, WFC
1997 Aug 15	43624	R	T	BATSE #6335, Konus, *RXTE*
1997 Dec 14	84041	R	T	BATSE #6533, Konus, *NEAR*, *RXTE*, WFC
1997 Dec 27	30187	R	R	BATSE #6546, Konus, WFC
1998 Jan 9	04346	R	R	BATSE #6564, Konus, WFC
1998 Mar 26	76733	R	T	BATSE #6660, Konus, WFC
1998 Mar 29	13478	T	T	BATSE #6665, COMPTEL, Konus, WFC
1998 Apr 25	78549	R	T	BATSE #6707, Konus, WFC
1998 May 19......	44412	R	R	BATSE #6764, Konus, WFC
1998 Jul 3	15765	R	T	BATSE #6891, *RXTE*
1998 Dec 20	78752	T	T	Konus, *RXTE*
1999 Jan 23	35216	R	T	BATSE #7343, COMPTEL, Konus, WFC
1999 May 10......	31746	R	R	BATSE #7560, Konus, *NEAR*, WFC

[a] Time at Earth.
[b] Konus: experiment aboard the *Wind* spacecraft. *DMSP*: *Defense Meteorological Satellite Program*. *RXTE*: *Rossi X-Ray Timing Explorer*. *NEAR*: *Near Earth Asteroid Rendezvous* mission.
[c] Recorded in triggered mode.
[d] Recorded in untriggered (real-time) mode.

angulation. These independent localizations include not only WFC observations, but also *BeppoSAX* Narrow-Field Instrument (NFI) pointings, optical and radio counterparts, and *Rossi X-Ray Timing Explorer* (*RXTE*) All-Sky Monitor detections. In all the cases considered here, the WFC and NFI observations preceded the Interplanetary Network (IPN) triangulation, and the IPN information was not used to determine the *BeppoSAX* pointing direction. Rather, the best source position available from the WFC observation was used to point the NFI; uncertainties in the WFC source position of several arcminutes are negligible compared with the NFI field of view.

Many of the bursts that satisfy these criteria have also been observed by other GRB instruments, notably BATSE and Konus (see Table 1). In some but not all cases, BATSE/*Ulysses* triangulation will result in somewhat more precise localizations than those presented here because of BATSE's larger area and better statistics. We defer these results to another paper.

TABLE 2

Third Interplanetary Network Annuli

Date	α(2000) (deg)	δ(2000) (deg)	Radius (deg)	δR (deg)	Δ (σ)
1997 Jan 11	177.732	+33.366	49.996	0.029	...
1997 Feb 28 ...	165.945	+36.526	83.423	0.009	2.05
1997 Apr 2	336.646	−35.576	64.726	2.694	0.006
1997 May 8	151.909	+32.056	51.227	0.145	0.20
1997 Aug 15 ...	159.651	+20.562	68.550	0.040	...
1997 Dec 14 ...	171.330	+11.721	53.737	0.041	0.86
1997 Dec 27 ...	170.783	+11.569	50.852	0.119	2.7
1998 Jan 9	349.654	−11.593	52.763	0.091	...
1998 Mar 26 ...	154.714	+13.166	40.778	0.043	2.1
1998 Mar 29 ...	154.299	+13.170	49.905	0.016	0.64
1998 Apr 25 ...	330.566	−12.778	49.670	0.428	0.30
1998 May 19...	329.485	−11.874	89.982	0.043	1.2
1998 Jul 3	331.648	−9.066	33.076	0.070	1.6
1998 Dec 20 ...	347.398	+7.338	67.120	0.005	...
1999 Jan 23	163.720	−9.464	81.346	0.010	0.48
1999 May 10...	144.802	−7.234	78.074	0.011	1.6

4. OBSERVATIONS AND RESULTS

Table 1 lists the dates, times, *Ulysses* and GRBM data modes, and the other experiments that observed the bursts. Table 2 gives the right ascension and declination of the centers of the IPN3 annuli, their radii, and their 3 σ half-widths. For those bursts for which an unambiguous counterpart was identified with greater precision than the annulus width, the last column in the table gives the angular distance Δ between the counterpart and the center line of the annulus, expressed in units of the number of σ of the

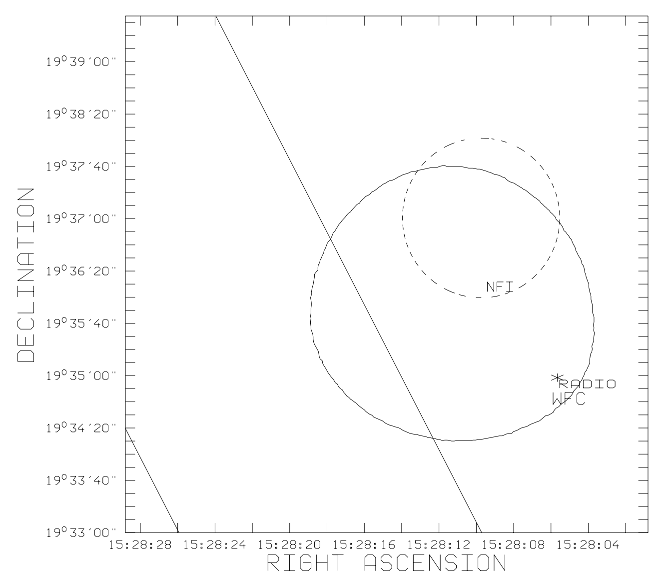

Fig. 1.—IPN3 annulus and the *BeppoSAX* WFC error box for GRB 970111. The NFI error circle (*dashed line*) indicates the position of a source believed to be unrelated to the GRB. The position of one of the radio sources reported by Galama et al. (1997) is also indicated.

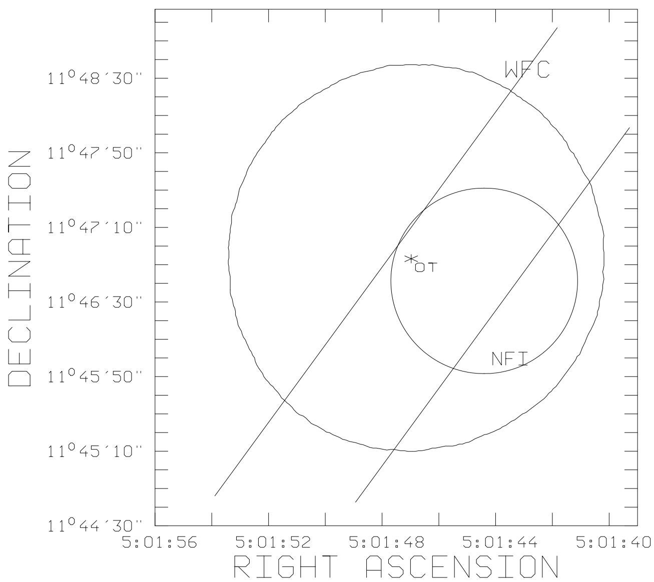

FIG. 2.—IPN3 annulus and the *BeppoSAX* WFC and NFI error boxes for GRB 970228. The position of the optical transient (van Paradijs et al. 1997) is also shown.

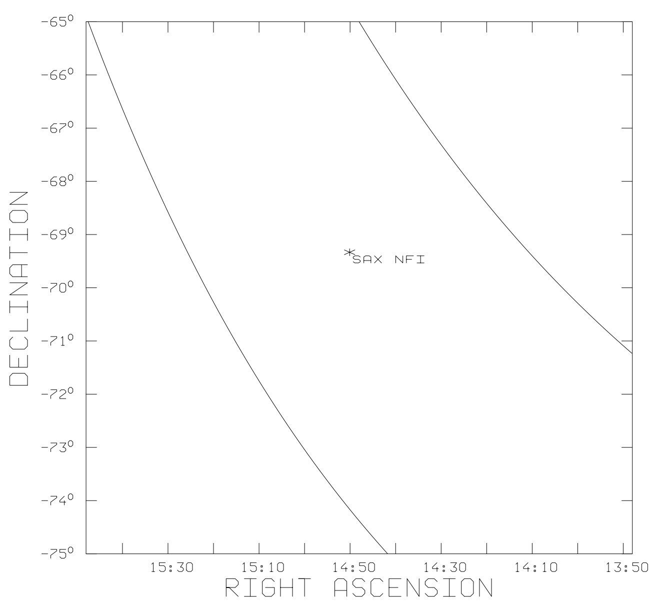

FIG. 3.—IPN3 annulus and the *BeppoSAX* NFI source for GRB 970402.

annulus width. Figures 1–16 show the localization maps. In all cases, the final *BeppoSAX* pointing directions have been used for the figures.

Figure 1 shows the IPN3 annulus and the *BeppoSAX* WFC error circle (Heise et al. 1998) for GRB 970111. (All the WFC error circles in this paper are 99% confidence, or 2.58 σ regions.) The NFI error circle (*dashed line*) indicates the position of a weak X-ray source. Since the source lies outside the annulus, this localization supports the hypothesis that the X-ray source and the burst are unrelated (Feroci et al. 1998). Two radio sources were detected in the vicinity of the WFC error box (Galama et al. 1997), one of which is shown in the figure (the other lies outside the boundaries). As neither displayed any fading behavior, they are not considered to be counterpart candidates. No fading optical sources were detected either.

Figure 2 shows the *BeppoSAX* WFC and NFI error circles for GRB 970228 (Heise et al. 1998; Costa et al. 1997). The IPN3 annulus was obtained from reprocessed *Ulysses* data and differs very slightly from the one in Hurley et al. (1997). The position of the fading optical counterpart is also shown (van Paradijs et al. 1997).

Figure 3 shows the IPN3 annulus for GRB 970402. This burst was quite weak and was detected only in the real-time, low-resolution data mode of *Ulysses*; although the GRBM triggered on it, the trigger occurred late in the event, and we have used the real-time data. A fading X-ray source was found in a *BeppoSAX* NFI observation (Nicastro et al. 1998a), but no optical counterpart was ever detected. *Ulysses* and GRBM time histories of this event are shown in Figure 17.

Figure 4 shows the IPN3 annulus, and the *BeppoSAX* WFC and NFI error circles for GRB 970508 (Heise et al. 1998; Piro et al. 1998a). The position of the optical counterpart is also indicated (Djorgovski et al. 1997). This burst too was quite weak, and although it triggered the *BeppoSAX* GRBM, it was observed only in the real-time data of *Ulysses*.

Figure 5 gives the IPN3 annulus and the *RXTE* error box for GRB 970815 (Smith et al. 1999). The *RXTE* error box is from the All-Sky Monitor and is defined by the response functions of two crossed collimators; the box therefore has equal probability per unit area everywhere. A slightly more precise IPN3 annulus, derived from BATSE and *Ulysses*, appears in Smith et al. (1999).

Figure 6 shows the IPN3 annulus and the *BeppoSAX* WFC (Heise et al. 1997) and NFI (Antonelli et al. 1997)

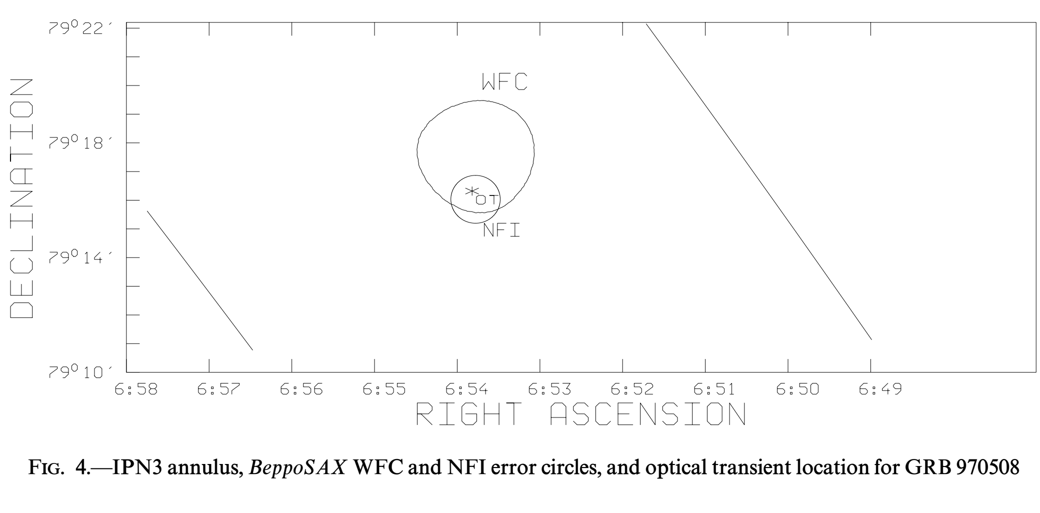

FIG. 4.—IPN3 annulus, *BeppoSAX* WFC and NFI error circles, and optical transient location for GRB 970508

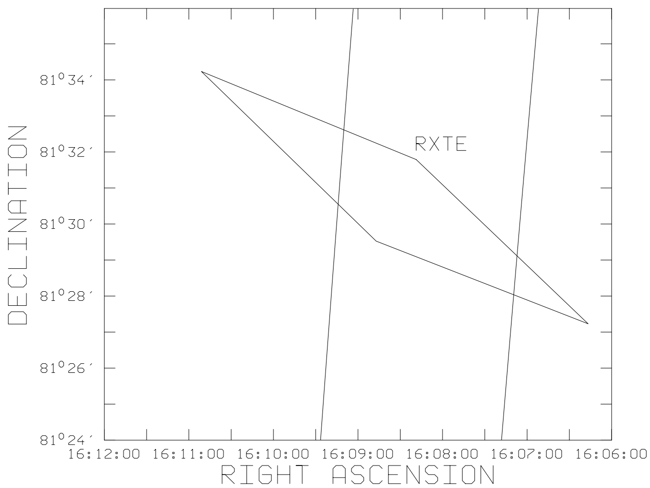

FIG. 5.—IPN3 annulus and *RXTE* error box for GRB 970815

error circles for GRB 971214. The position of the optical counterpart (Halpern et al. 1998) is also shown. IPN3 and *RXTE* locations appeared in Kippen et al. (1997).

Figure 7 gives the IPN3 annulus and the *BeppoSAX* WFC (Coletta et al. 1997) error circle for GRB 971227. The burst was weak and was detected only marginally by *Ulysses*, and it was detected in the real-time data of the GRBM. Consequently, the annulus is subject to rather large systematic uncertainties. A weak X-ray source detected at the 4 σ level in an NFI observation has been proposed as the fading X-ray counterpart by Piro et al. (1997) and Antonelli et al. (1999). No radio or optical counterpart was identified. The WFC error box is large because of poor attitude reconstruction for this event.

Figure 8 gives the IPN3 annulus and the *BeppoSAX* WFC (in 't Zand et al. 1998a) error circle for GRB 980109; no NFI observation was carried out, because of the relatively large uncertainty in the WFC localization (again because of poor attitude reconstruction). A possible optical counterpart was initially identified, but is no longer considered to be related to the GRB (E. Pian & T. Galama 1999, private communication). It lay within the preliminary IPN3 annulus, but it lies just outside the final one.

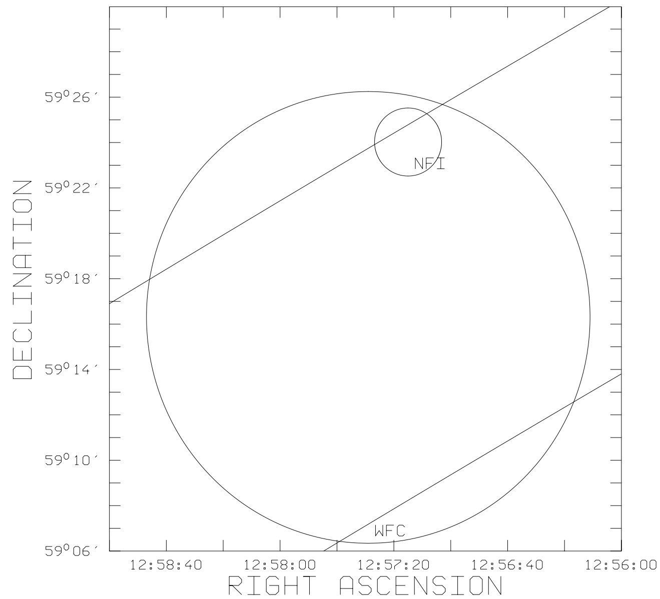

FIG. 7.—IPN3 annulus and *BeppoSAX* WFC and NFI error circles for GRB 971227.

Figure 9 shows the IPN3 annulus and the *BeppoSAX* WFC error circle (Celidonio et al. 1998) for GRB 980326. No NFI observations were carried out, but Groot et al. (1997) identified an optical transient in the WFC error circle. A preliminary IPN3 annulus appeared in Hurley (1998a).

Figure 10 gives the IPN3 annulus and the *BeppoSAX* WFC (Frontera et al. 1998) and NFI (in 't Zand et al. 1998b) error circles for GRB 980329. A radio counterpart was identified by Taylor et al. (1998), and an optical counterpart was found at the same position by Palazzi et al. (1998). A preliminary IPN3 annulus appeared in Hurley (1998b).

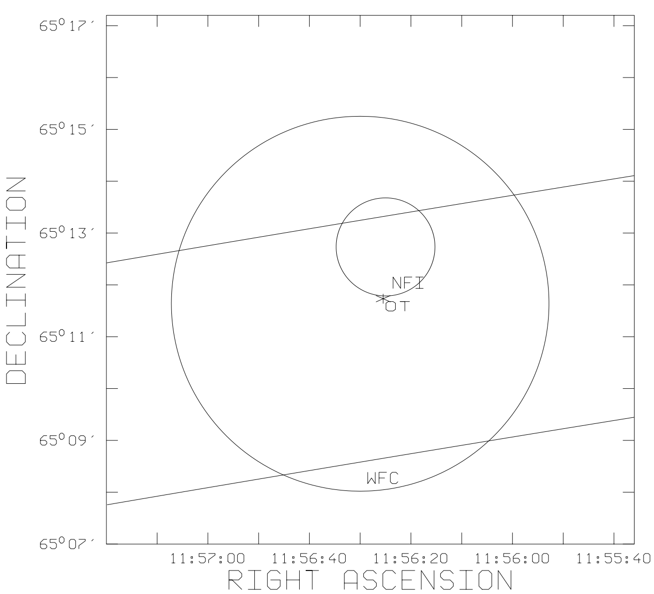

FIG. 6.—IPN3 annulus, *BeppoSAX* WFC and NFI error circles, and optical transient location for GRB 971214.

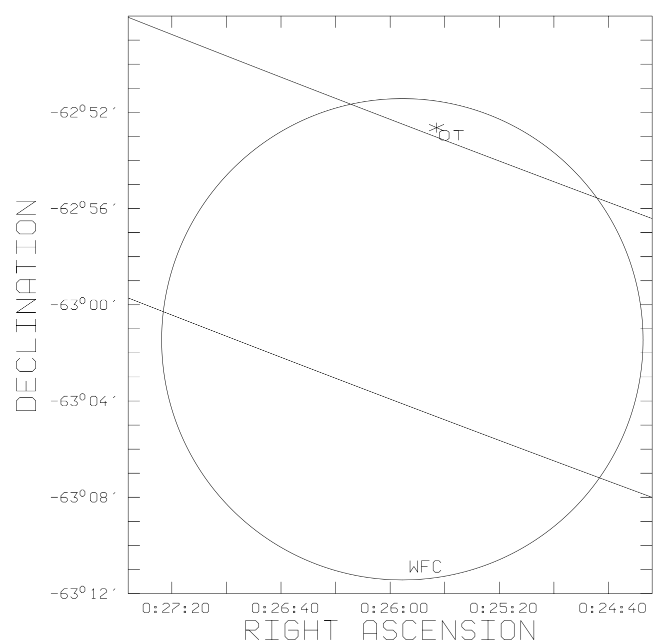

FIG. 8.—IPN3 annulus, *BeppoSAX* WFC error circle, and possible optical counterpart of GRB 980109.

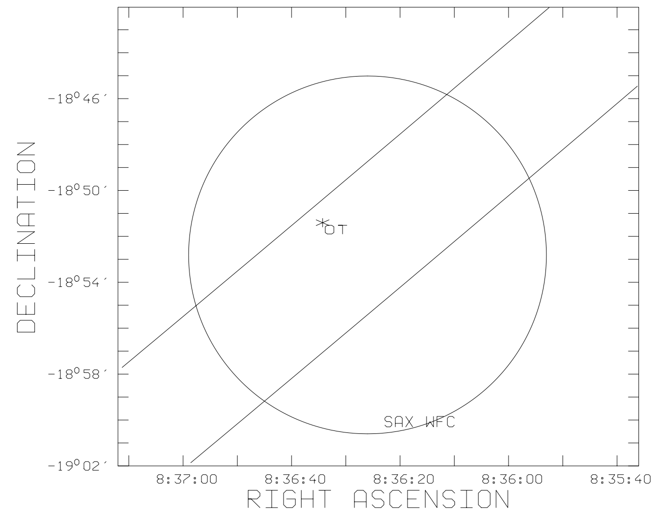

FIG. 9.—IPN3 annulus, *BeppoSAX* WFC error circle, and optical transient location for GRB 980326.

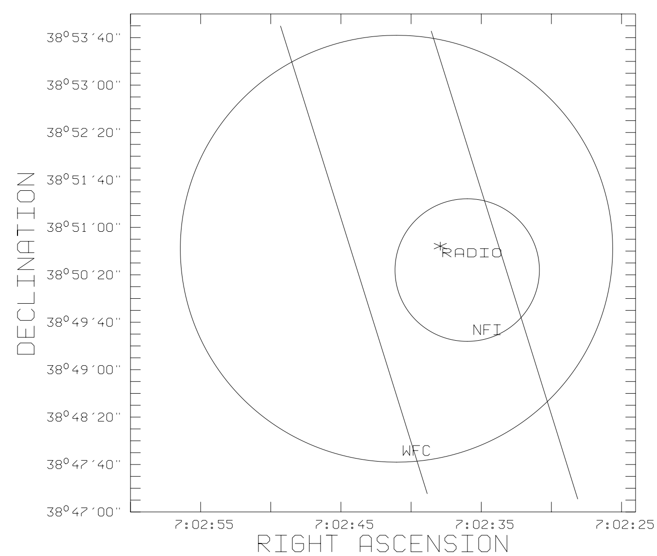

FIG. 10.—IPN3 annulus, *BeppoSAX* WFC and NFI error circles, and radio counterpart location for GRB 980329. The optical counterpart location is the same as that of the radio counterpart.

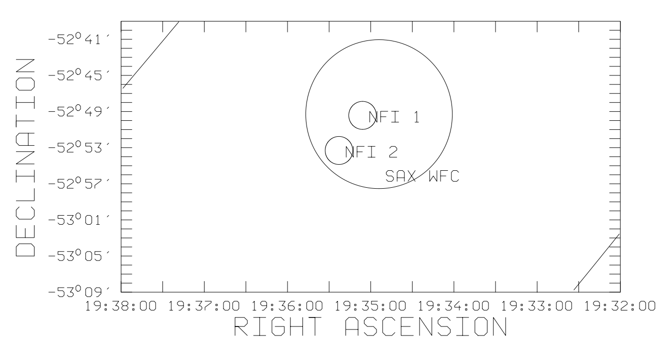

FIG. 11.—IPN3 annulus (*upper left corner* and *lower right corner*) and the *BeppoSAX* WFC and NFI error circles for GRB 980425. NFI source 1 is associated with SN1998bw.

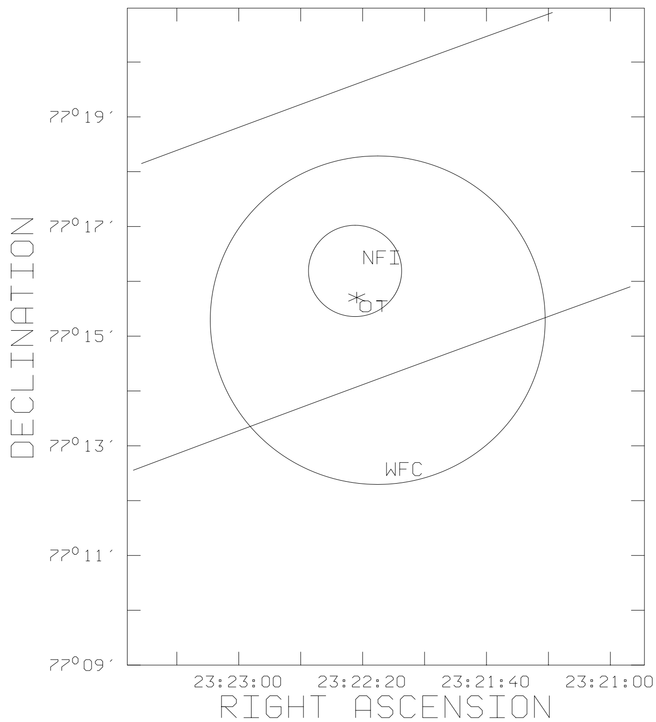

FIG. 12.—IPN3 annulus, *BeppoSAX* WFC and NFI error circles, and optical transient position for GRB 980519.

Figure 11 shows the IPN3 annulus and the *BeppoSAX* WFC (Soffitta et al. 1998) and the two revised NFI (Piro et al. 1998b) error circles for GRB 980425. The position of source 1 is consistent with that of the unusual supernova 1998bw (Galama et al. 1998a). However, because the burst was weak, it was detected only in the *Ulysses* real-time data, and the IPN3 annulus is wide; it cannot be used to determine which NFI source is associated with the GRB.

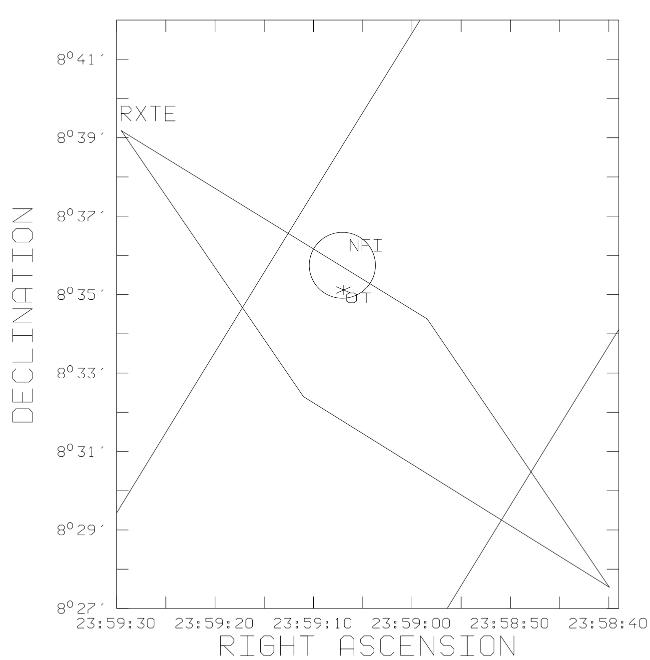

FIG. 13.—IPN3 annulus, *RXTE* error box, *BeppoSAX* NFI error circle, and position of the optical transient and radio counterpart of GRB 980703.

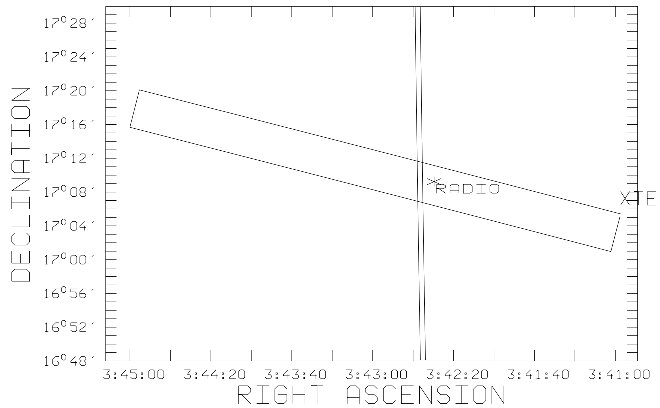

FIG. 14.—IPN3 annulus, *RXTE* error box, and position of radio source for GRB 981220.

Figure 12 shows the IPN3 annulus, the *BeppoSAX* WFC (Muller et al. 1998) and NFI (Nicastro et al. 1998b) error circles, and the position of the optical transient (Hjorth 1998) for GRB 980519.

Figure 13 shows the IPN3 annulus, the *RXTE* error box (Smith et al. 1999), the NFI source location (Vreeswijk et al. 1999), and the position of the optical and radio counterparts (Bloom et al. 1998) for GRB 980703. This annulus is consistent with, but narrower than, the initial BATSE/*Ulysses* annulus (Hurley & Kouveliotou 1998). As for GRB 970815, the *RXTE* error box is from the All-Sky Monitor and is defined by the response functions of two crossed collimators; the box therefore has equal probability per unit area everywhere.

Figure 14 shows the IPN3 annulus and the *RXTE*/ASM error box (Smith et al. 1999) for GRB 981220. A radio source was proposed as a possible counterpart (Galama et al. 1998b; Frail & Kulkarni 1998) but is no longer thought to be related to the GRB (Frail, Kulkarni, & Taylor 1999; Hurley & Feroci 1999). A preliminary annulus has appeared in Hurley et al. (1999b).

Figure 15 shows the IPN3 annulus, the *BeppoSAX* WFC (Feroci et al. 1999) and NFI (Heise et al. 1999) error circles, and the position of the optical transient (Akerlof et al. 1999)

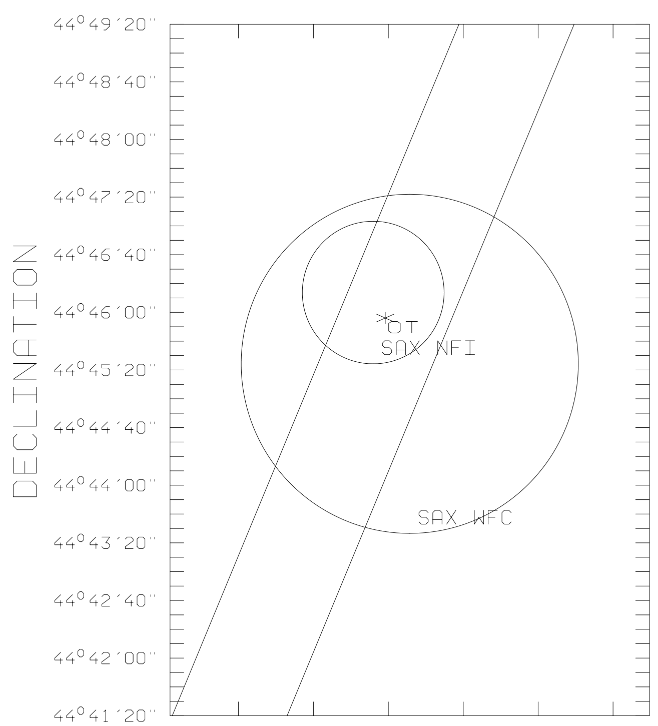

FIG. 15.—IPN3 annulus, *BeppoSAX* WFC and NFI error circles, and optical transient position for GRB 990123.

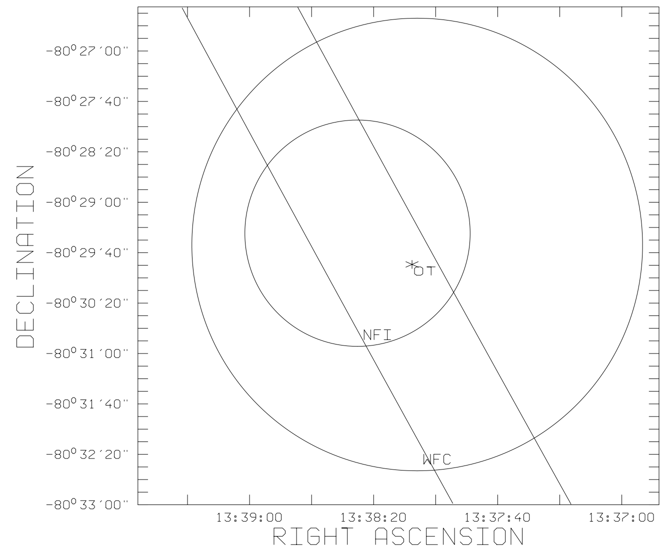

FIG. 16.—IPN3 annulus, *BeppoSAX* WFC and NFI error circles, and optical transient position for GRB 990510.

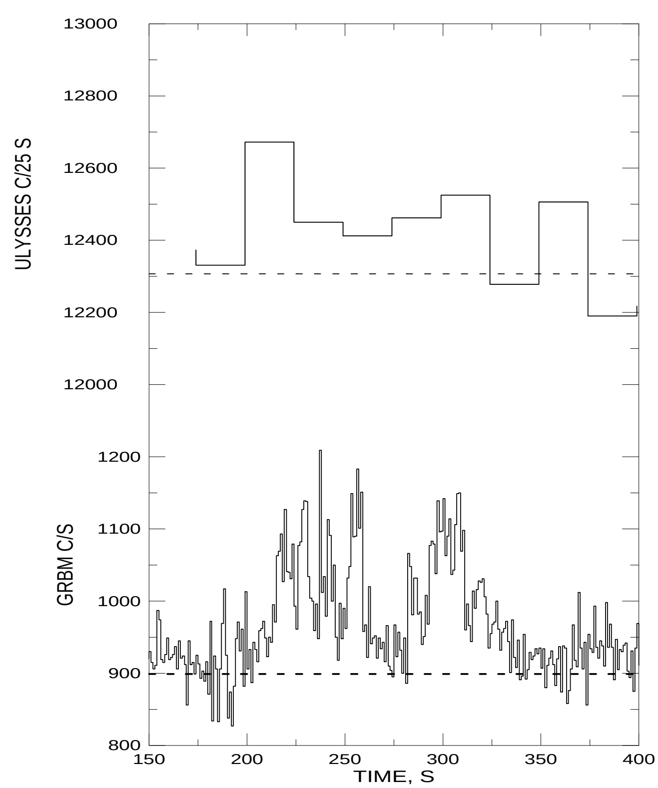

FIG. 17.—*Ulysses* (*top*) and GRBM (*bottom*) time histories of GRB 970402. Both instruments observed the burst in real-time data modes. The *Ulysses* data have been regrouped to 25 s resolution to improve statistics. Dashed lines indicate the background levels.

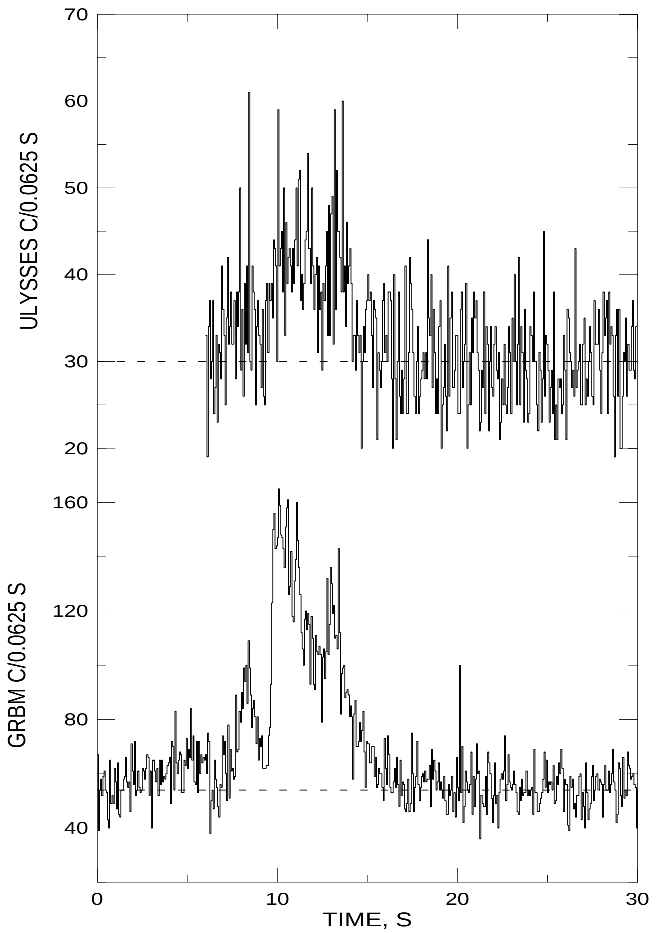

FIG. 18.—*Ulysses* (*top*) and GRBM (*bottom*) time histories of GRB 981220. Both instruments observed this event in triggered data modes. Dashed lines indicate the background levels.

for GRB 990123. A preliminary IPN3 annulus was circulated in Hurley (1999).

Figure 16 shows the IPN3 annulus, the *BeppoSAX* WFC (Dadina et al. 1999) and NFI (Kuulkers et al. 1999) error circles, and the position of the optical transient (Galama et al. 1999) for GRB 990510.

We have selected the light curves of two bursts that were not observed by BATSE for display in Figures 17 and 18. These show the GRBM and *Ulysses* real-time and triggered data.

5. DISCUSSION

The *BeppoSAX* GRBM is clearly a sensitive burst detector that makes an important contribution to the IPN3 by providing high-quality data for events that are not observed by BATSE. This is the case for three of the bursts discussed here. (This number is fewer than would have been predicted, based on a probability of 48% that BATSE will detect any burst above its threshold [Paciesas et al. 1999]; however, some of the events in this paper were in effect selected because of the knowledge of their detection by BATSE.) We have demonstrated that, despite the very different properties of the GRBM and the *Ulysses* GRB experiment, very accurate triangulations can be done. In the case of bright bursts, these annuli can be used to reduce or further constrain the WFC and NFI error boxes.

K. H. is grateful to JPL for *Ulysses* support under Contract 958056 and to the NASA Astrophysics Data Program for supporting the integration of *BeppoSAX* into the IPN3 under NAG5-7766. *BeppoSAX* is a program of the Italian Space Agency, with participation of NIVR, the Dutch Space Agency.

REFERENCES

Akerlof, C., et al. 1999, Nature, 398, 400
Amati, L., et al. 1997, Proc. SPIE, 3114, 176
Antonelli, L., et al. 1997, IAU Circ. 6792
———. 1999, A&A, 138, 435
Bloom, J., et al. 1998, ApJ, 508, L21
Celidonio, G., et al. 1998, IAU Circ. 6851
Coletta, A., et al. 1997, IAU Circ. 6796
Costa, E., et al. 1997, Nature, 387, 783
Dadina, M., et al. 1999, IAU Circ. 7160
Djorgovski, S., et al. 1997, Nature, 387, 876
Feroci, M., et al. 1997, Proc. SPIE, 3114, 186
———. 1998, A&A, 332, L29
———. 1999, IAU Circ. 7095
Frail, D., & Kulkarni, S. 1998, GCN Circ. 170 (http://gcn.gsfc.nasa.gov/gcn/gcn3/170.gcn3)
Frail, D., Kulkarni, S., & Taylor, G. 1999, GCN Circ. 269 (http://gcn.gsfc.nasa.gov/gcn/gcn3/269.gcn3)
Frontera, F., et al. 1997, A&AS, 122, 357
Frontera, F., Costa, E., Piro, L., Soffitta, P., in 't Zand, J., di Ciolo, L., Tesseri, A., & Smith, M. 1998, IAU Circ. 6853
Galama, T., et al. 1997, ApJ, 486, L5
———. 1998a, Nature, 395, 670
———. 1998b, GCN Circ. 168 (http://gcn.gsfc.nasa.gov/gcn/gcn3/168.gcn3)
———. 1999, GCN Circ. 310 (http://gcn.gsfc.nasa.gov/gcn/gcn3/310.gcn3)
Groot, P., et al. 1997, ApJ, 502, L123
Halpern, J., et al. 1998, Nature, 393, 41
Heise, J., et al. 1997, IAU Circ. 6787
———. 1998, in AIP Conf. Proc. 428, 4th Huntsville Symp. on Gamma-Ray Bursts, ed. C. Meegan, R. Preece, & T. Koshut (New York: AIP), 397
Heise, J., de Libero, C., Daniele, M., Scotti, G., Ricci, D., Capalbi, M., Antonelli, L., & Costa, E. 1999, IAU Circ. 7099
Hjorth, J. 1998, GCN Circ. 78 (http://gcn.gsfc.nasa.gov/gcn/gcn3/078.gcn3)
Hurley, K. 1998a, GCN Circ. 53 (http://gcn.gsfc.nasa.gov/gcn/gcn3/053.gcn3)
Hurley, K. 1998b, GCN Circ. 49 (http://gcn.gsfc.nasa.gov/gcn/gcn3/049.gcn3)
———. 1999, GCN Circ. 222 (http://gcn.gsfc.nasa.gov/gcn/gcn3/222.gcn3)
Hurley, K., et al. 1992, A&AS, 92, 401
———. 1997, ApJ, 485, L1
Hurley, K., Briggs, M., Kippen, R., Kouveliotou, C., Meegan, C., Fishman, G., Cline, T., & Boer, M. 1999a, ApJS, 120, 399
Hurley, K., Cline, T., Mazets, E., & Golenetskii, S. 1999b, GCN Circ. 160 (http://gcn.gsfc.nasa.gov/gcn/gcn3/160.gcn3)
Hurley, K., & Feroci, M. 1999, GCN Circ. 270 (http://gcn.gsfc.nasa.gov/gcn/gcn3/270.gcn3)
Hurley, K., & Kouveliotou, C. 1998, GCN Circ. 125 (http://gcn.gsfc.nasa.gov/gcn/gcn3/125.gcn3)
in 't Zand, J., et al. 1998a, IAU Circ. 6805
———. 1998b, IAU Circ. 6854
Kippen, R., Woods, P., Connaughton, V., Smith, D., Levine, A., Remillard, R., & Hurley, K. 1997, IAU Circ. 6789
Kuulkers, E., et al. 1999, GCN Circ. 326 (http://gcn.gsfc.nasa.gov/gcn/gcn3/326.gcn3)
Muller, J., Heise, J., Frontera, F., Di Ciolo, L., Gandolfi, G., Coletta, A., & Soffitta, P. 1998, IAU Circ. 6910
Nicastro, L., et al. 1998a, A&A, 338, L17
Nicastro, L., Antonelli, L., Celidonio, G., Daniele, M., de Libero, C., Spoliti, G., Prio, L., & Pian, E. 1998b, IAU Circ. 6912
Paciesas, W., et al. 1999, ApJS, 122, 465
Palazzi, E., et al. 1998, A&A, 336, L95
Piro, L., et al. 1997, IAU Circ. 6797
———. 1998a, A&A, 331, L41
Piro, L., Butler, R., Fiore, F., Antonelli, A., & Pian, E. 1998b, GCN Circ. 155 (http://gcn.gsfc.nasa.gov/gcn/gcn3/155.gcn3)
Smith, D., et al. 1999, ApJ, 526, 683
Soffitta, P., et al. 1998, IAU Circ. 6884
Taylor, G., Frail, D., Kulkarni, S., Shepherd, D., Feroci, M., & Frontera, F. 1998, ApJ, 502, L115
van Paradijs, J., et al. 1997, Nature, 386, 686
Vreeswijk, P., et al. 1999, ApJ, 523, 171